1-1-2012

Generalised diffusive delay logistic equations: Semi-analytical solutions

H Y. Alfifi
University of Wollongong, hyja973@uow.edu.au

Timothy R. Marchant
University of Wollongong, tim@uow.edu.au

M I. Nelson
University of Wollongong, mnelson@uow.edu.au

Generalised diffusive delay logistic equations: Semi-analytical solutions

Abstract

This paper considers semi-analytical solutions for a class of generalised logis- tic partial dierential equations with both point and distributed delays. Both one and two-dimensional geometries are considered. The Galerkin method is used to approximate the governing equations by a system of ordinary dierential delay equations. This method involves assuming a spatial structure for the solution and averaging to obtain the ordinary dierential delay equation models. Semi-analytical results for the stability of the system are derived with the critical parameter value, at which a Hopf bifurcation occurs, found. The results show that diusion acts to stabilise the system, compared to equivalent non- diusive systems and that large delays, which represent feedback from the distant past, act to destabilize the system. Comparisons between semi-analytical and numerical solutions show excellent agreement for steady state and transient solutions, and for the parameter values at which the Hopf bifurcations occur.

Keywords

analytical, generalised, diffusive, delay, logistic, equations, semi, solutions

Disciplines

Physical Sciences and Mathematics

Publication Details

Alfifi, H. Y., Marchant, T. R. & Nelson, M. I. (2012). Generalised diffusive delay logistic equations: Semi-analytical solutions. Dynamics of Continuous, Discrete and Impulsive Systems Series B: Applications and Algorithms, 19 (4-5), 579-596.

Dynamics of Continuous, Discrete and Impulsive Systems
Series B: Applications & Algorithms 19 (2012) 579-596
 http://www.watsci.org

GENERALISED DIFFUSIVE DELAY LOGISTIC EQUATIONS: SEMI-ANALYTICAL SOLUTIONS

H.Y. Alfifi, T.R. Marchant and M.I. Nelson

School of Mathematics and Applied Statistics, The University of Wollongong, Wollongong, 2522, N.S.W., Australia.

Corresponding author email: tim_marchant@uow.edu.au.

Abstract. This paper considers semi-analytical solutions for a class of generalised logistic partial differential equations with both point and distributed delays. Both one and two-dimensional geometries are considered. The Galerkin method is used to approximate the governing equations by a system of ordinary differential delay equations. This method involves assuming a spatial structure for the solution and averaging to obtain the ordinary differential delay equation models. Semi-analytical results for the stability of the system are derived with the critical parameter value, at which a Hopf bifurcation occurs, found. The results show that diffusion acts to stabilise the system, compared to equivalent non-diffusive systems and that large delays, which represent feedback from the distant past, act to destabilize the system. Comparisons between semi-analytical and numerical solutions show excellent agreement for steady state and transient solutions, and for the parameter values at which the Hopf bifurcations occur.

Keywords. semi-analytical solutions; reaction-diffusion-delay equations; logistic equation; Hopf bifurcations; distributed delay.

AMS (MOS) subject classification: 35,37,41.

1 Introduction

Differential delay equations have been studied extensively and arise in a variety of biological, chemical and physical applications. The introduction of a delay into the governing equation can introduce instability, via a Hopf bifurcation, with the subsequent development of limit cycles (periodic solutions). [12] reviewed delay equations for a range of engineering applications, including feedback systems involving sensors or actuators, neural networks in the brain, high speed milling, laser dynamics, and traffic dynamics. Many population, biological and chemical applications, modeled by delay equations, are described in [4]. Applications described include Nicholson's blowfly model, autoimmune diseases, genetic oscillations and thermochemical reactions.

The logistic equation describes a simple population growth model which, due to limited resources or competition, reaches a stable steady-state population. [10] introduced a delay into the competition term and obtained the

delay logistic equation

$$\frac{du}{dt} = \lambda u(t)(1 - u(t-1)), \tag{1}$$

which has a steady-state solution for $0 < \lambda < \frac{\pi}{2}$ and periodic solutions for $\lambda > \frac{\pi}{2}$, see [4]. Equation (1) has been considered by many authors,[1, 2, 3, 6, 19].

[6] found an asymptotic solution to the delay logistic equation, for the case when the delay is large. He derived explicit expressions describing the periodic solution, including the period and the maximum and minimum amplitudes. A good comparison was found between the analytical and numerical solutions, for large λ. [7] extended the asymptotic techniques to other delay equations, including the delayed recruitment equation, a model of stem-cell renewal and density wave oscillations in boilers.

[15] considered a generalised logistic equation with distributed delay. The form of distributed delay considered allowed the generalised delay equation to be written as a set of two coupled point delay equations. Explicit expressions were obtained for the occurrence of Hopf bifurcations. [18] considered the generalised logistic equation, with the delays weighted by an exponential function. Again the equation was written as a set of coupled point delay equations, for which the stability is determined using standard techniques.

There are many applications where the effects of diffusion are also important and a reaction-diffusion-delay equation is the appropriate model. Some applications from population ecology include [5, 8, 11, 17]. [20] considered a coupled set of reaction-diffusion-delay equations which model cellular neural networks. They proved results relating to existence and uniqueness of the steady-state solution and the existence of periodic solutions. For reaction-diffusion equations the standard techniques of combustion theory cannot be applied. In [13] a semi-analytical method was used to examine the Gray Scott cubic autocatalytic scheme in a reaction-diffusion cell. This involved approximating the governing partial differential equations (pdes) by ordinary differential equations (odes). The semi-analytical model was then analysed by combining a local stability analysis and singularity theory to determine the regions of parameter space in which the various bifurcation patterns and Hopf bifurcations occurred. An excellent comparison was obtained between the semi-analytical results and numerical solutions of the governing pdes.

In [14] semi-analytical solutions for one- and two-dimensional porous catalytic pellets were developed. As the Arrhenius reaction term cannot be integrated explicitly, the semi-analytical model consisted of integro-differential equations. Both the static and dynamic stability of the pellets were investigated and highly accurate solutions were obtained. The semi-analytical model was then analysed using a stability analysis and singularity theory to determine the regions in which Hopf bifurcations occurred. An excellent comparison was achieved between the numerical and semi-analytical solutions.

In this paper a generalised diffusive delay logistic equation, is considered. The governing pde is approximated by an ode model, using the Galerkin

technique considered by [13, 14]. This allows approximate bifurcation diagrams be found while a stability analysis of the delay ode model then allows approximations, for the parameter range for which Hopf bifurcations occur, to be obtained.

In Section 2 we formulate both point delay and distributed delay problems. For the distributed delay both uniformly weighted and exponentially weighted delays are considered. In Section 3 the semi-analytical ode model is derived and in Section 4 steady-state solutions are found. Section 5 presents a stability analysis to determine the Hopf bifurcation points. In Section 6 comparisons are made between semi-analytical and numerical solutions, of bifurcation diagrams and transient solutions.

2 Problem formulation

The diffusive delay logistic pde, for a two-dimensional geometry, is written as

$$u_t = \nabla^2 u + \lambda u \left(1 - \frac{1}{\int_0^\tau f(p)\, dp} \int_0^\tau f(p) u(t-p)\, dp\right), \qquad (2)$$
$$u = 0, \quad \text{at} \quad x = \pm 1, \quad y = \pm 1, \quad u = u_a, \quad -\tau < t \leq 0$$

We term the variable u as the population density even through (2) has applications besides population modeling and explicitly write the time dependence of u only when a delay is present in that term. The boundary conditions in (2) are fixed hence, it is an open system. The generalised delay term is distributed over a time interval of length τ and weighted by f. λ is the growth or proliferation rate and the initial condition represents a constant population u_a for $t \in (-\tau, 0)$. We let

$$v = \frac{1}{\int_0^\tau f(p)\, dp} \int_0^\tau f(p) u(t-p)\, dp, \quad v = u_a \quad \text{at} \quad t = 0, \qquad (3)$$

We consider three examples in detail. A point delay system, a uniformly weighted delay and an exponentially weighted delay. For the point delay system we let the weighting function $f(p) = \delta(p - \tau)$, which implies $v(t) = u(t - \tau)$, and the point delay pde

$$u_t = \nabla^2 u + \lambda u \left(1 - u(t-\tau)\right), \qquad (4)$$

is obtained. We also consider an exponential weighting function, $f(p) = e^{-\gamma p}$. This gives

$$v = \frac{1}{\int_0^\tau e^{-\gamma p}\, dp} \int_0^\tau u(t-p)\, e^{-\gamma p}\, dp. \qquad (5)$$

Using the linear chain trick (see [18]) on (5), the governing equations can be written as a coupled pde-ode system involving only point delays,

$$u_t = \nabla^2 u + \lambda u(1 - v), \quad v_t = \frac{\gamma(u - u(t-\tau)e^{-\gamma\tau})}{(1 - e^{-\gamma\tau})} - \gamma v. \qquad (6)$$

We study two examples in detail, $\gamma = 0$, which represents a uniformly weighted delay, and a special case of exponentially weighted delay, $\gamma = 1$. Note, to obtain the ode for v in the $\gamma = 0$ case, (6) must be expanded in a Taylor series, for small γ. A Crank-Nicholson finite-difference scheme is used to find the numerical solutions of the governing pdes, for the different delay cases, while the ode is solved using a fourth-order Runge-Kutta method.

3 The Galerkin method

Equation (2) is solved using a Galerkin method, which assumes a spatial structure for the population density profile [14]. The Galerkin method allows the governing pdes to be approximated by odes. Besides the examples considered in this paper we note that the Galekin method is suitable for general weighing functions f, for which an explicit point delay form, such as (4) and (6), is not available.

The one-dimensional models use the expansion

$$u(x,t) = u_0(t)\cos\left(\frac{\pi}{2}x\right) + u_1(t)\cos\left(\frac{3\pi}{2}x\right). \tag{7}$$

Equation (7) satisfies the boundary conditions described in (2), but not the governing pdes. The coefficients in (7) are obtained by evaluating averaged versions of governing equations, weighted by the basis functions $\cos\left(\frac{1}{2}\pi x\right)$ and $\cos\left(\frac{3}{2}\pi x\right)$. The ode system is

$$\begin{aligned}
\frac{du_0}{dt} &= -\frac{\pi^2}{4}u_0 + \lambda(u_0 - \frac{8}{3\pi}u_0v_0 - \frac{8}{15\pi}u_1v_0 - \frac{8}{15\pi}v_1u_0 - \frac{72}{35\pi}u_1v_1),\\
\frac{du_1}{dt} &= -\frac{9\pi^2}{4}u_1 + \lambda(u_1 - \frac{8}{15\pi}u_0v_0 - \frac{72}{35\pi}u_1v_0 - \frac{72}{35\pi}u_0v_1 + \frac{8}{9\pi}u_1v_1),\\
v_i(t) &= \frac{1}{\int_0^\tau f(p)\,dp}\int_0^\tau f(p)u_i(t-p)dp, \quad i = 0, 1.
\end{aligned} \tag{8}$$

The series in (8) has been truncated after two terms. This is due to the fact that the number of terms that are required to be included in the truncated series represents a trade-off between the accuracy and complexity of the semi-analytical solution. It will be seen later that a two-term method gives enough accuracy without extreme expression swell. Furthermore the one term solution can be calculated when $u_1 = 0$.

For the two-dimensional models, the expansion

$$\begin{aligned}
u(x,y,t) = {} & u_0(t)\cos\left(\frac{\pi}{2}x\right)\cos\left(\frac{\pi}{2}y\right) + u_1(t)\cos\left(\frac{3\pi}{2}x\right)\cos\left(\frac{\pi}{2}y\right)\\
& + u_1(t)\cos\left(\frac{\pi}{2}x\right)\cos\left(\frac{3\pi}{2}y\right) + u_2(t)\cos\left(\frac{3\pi}{2}x\right)\cos\left(\frac{3\pi}{2}y\right),
\end{aligned} \tag{9}$$

is used, which satisfies the boundary conditions in (2). The expansions in (9) have four terms, but symmetry implies that two of the terms have the same coefficient. The equation in (9) is weighted by the basis functions $\cos(\frac{1}{2}\pi x)\cos(\frac{1}{2}\pi y)$, $\cos(\frac{1}{2}\pi x)\cos(\frac{3}{2}\pi y)$, $\cos(\frac{3}{2}\pi x)\cos(\frac{3}{2}\pi y)$ in turn, to obtain the ode system,

$$
\begin{aligned}
\frac{du_0}{dt} &= -\frac{\pi^2}{2}u_0 + \lambda(u_0 - \frac{64}{9\pi^2}u_0v_0 - \frac{128}{45\pi^2}u_1v_0 - \frac{128}{45\pi^2}u_0v_1) \\
&- \lambda(\frac{64}{255\pi^2}u_0v_2 + \frac{64}{255\pi^2}u_2v_0 + \frac{5184}{1225\pi^2}u_2v_2 + \frac{384}{175\pi^2}u_2v_1) \\
&- \lambda(\frac{18176}{1575\pi^2}u_1v_1 + \frac{384}{175\pi^2}u_1v_2), \\
\frac{du_1}{dt} &= -\frac{5\pi^2}{2}u_1 + \lambda(u_1 - \frac{64}{45\pi^2}u_0v_0 - \frac{192}{175\pi^2}u_0v_2 + \frac{64}{35\pi^2}u_2v_2) \\
&- \lambda(\frac{192}{175\pi^2}u_2v_0 + \frac{124288}{33075\pi^2}u_1v_2 + \frac{124288}{33075\pi^2}u_2v_1 + \frac{9088}{1575\pi^2}u_1v_0) \\
&- \lambda(\frac{9088}{1575\pi^2}u_0v_1 + \frac{4352}{4725\pi^2}u_1v_1), \\
\frac{du_2}{dt} &= -\frac{9\pi^2}{2}u_2 + \lambda(u_2 - \frac{64}{255\pi^2}u_0v_0 + \frac{128}{35\pi^2}u_2v_1 - \frac{64}{81\pi^2}u_2v_2) \\
&+ \lambda(\frac{128}{35\pi^2}u_1v_2 - \frac{5184}{1225\pi^2}u_0v_2 - \frac{5184}{1225\pi^2}u_2v_0 - \frac{384}{175\pi^2}u_1v_0) \\
&- \lambda(\frac{384}{175\pi^2}u_0v_1 + \frac{248576}{33075\pi^2}u_1v_1), \\
v_i(t) &= \frac{1}{\int_0^\tau f(p)\,dp}\int_0^\tau f(p)u_i(t-p)dp, \quad i = 0,1,2.
\end{aligned}
\tag{10}
$$

4 Steady-state solutions

In this section we consider the steady-state solutions of the delay differential model for the one and two dimensional geometries. We let $u_i(t) = u_i(t-\tau) = v_i(t) = u_i$ and the ode model reduces to sets of transcendental equations. For the one dimensional case the steady-state solution is given by

$$
\begin{aligned}
f_1 = &\quad -\frac{\pi^2}{4\lambda}u_0 + u_0 - \frac{8}{3\pi}u_0^2 - \frac{72}{35\pi}u_1^2 - \frac{16}{15\pi}u_0u_1 = 0, \\
f_2 = &\quad -\frac{\pi^2}{9\lambda}u_1 + u_1 - \frac{8}{15\pi}u_0^2 + \frac{8}{9\pi}u_1^2 - \frac{144}{35\pi}u_0u_1 = 0.
\end{aligned}
\tag{11}
$$

while in the two dimensional case, we obtain

$$\begin{aligned}
f_1 &= -\frac{\pi^2}{2\lambda}u_0 + u_0 - \frac{64}{9\pi^2}u_0^2 - \frac{18176}{1575\pi^2}u_1^2 - \frac{5184}{1225\pi^2}u_2^2 \\
&\quad -\frac{256}{45\pi^2}u_0u_1 - \frac{128}{225\pi^2}u_0u_2 - \frac{768}{175\pi^2}u_1u_2 = 0, \\
f_2 &= -\frac{5\pi^2}{2\lambda}u_1 + u_1 - \frac{64}{45\pi^2}u_0^2 - \frac{4352}{4725\pi^2}u_1^2 + \frac{64}{35\pi^2}u_2^2 \\
&\quad -\frac{18176}{1575\pi^2}u_0u_1 - \frac{384}{175\pi^2}u_0u_2 - \frac{248576}{33075\pi^2}u_1u_2 = 0, \\
f_3 &= -\frac{9\pi^2}{2\lambda}u_2 + u_2 - \frac{64}{255\pi^2}u_0^2 - \frac{248576}{33075\pi^2}u_1^2 - \frac{64}{81\pi^2}u_2^2 \\
&\quad -\frac{768}{175\pi^2}u_0u_1 - \frac{10368}{1225\pi^2}u_0u_2 + \frac{256}{35\pi^2}u_1u_2 = 0.
\end{aligned} \tag{12}$$

The steady-state solutions for the one and two-dimensional models are given by the solution to the equations $f_i = 0$. These are found numerically, using a root-finding routine in the MAPLE package. Note that the steady-state solutions of (2) are the same for all choices of delay weighting function, f.

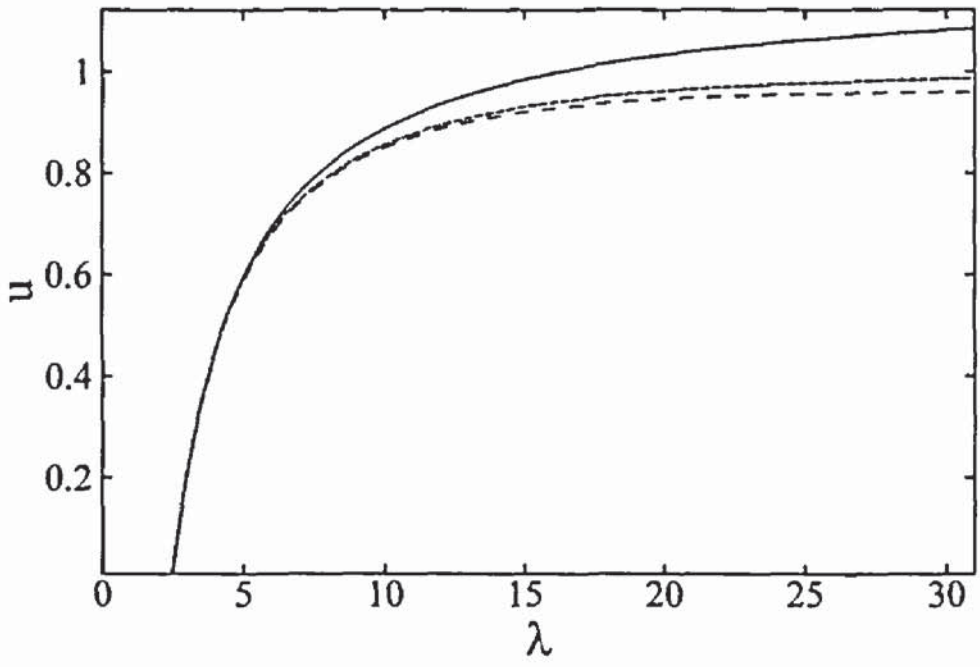

Figure 1: The steady-state population density u, at $x = 0$, for the one-dimensional model. Shown is the one-term (solid line) and two-term (long dashes) semi analytical solutions of (2) and numerical (small dashes) solutions of (13).

Figure 1 shows the steady-state population density u at $x = 0$, for the one-dimensional model. Shown are the one and two-term semi-analytical solutions of (2) and numerical solutions of (13) at the centre of the domain,

$x = 0$. The non-uniform steady-state solution bifurcates from the uniform $u = 0$ solution at $\lambda = \frac{\pi^2}{4}$ and increases exponentially, as λ increases, before approaching a maximum population density of $u \simeq 1$. Note that the presented numerical solutions are of the Fisher equation,

$$u_t = \nabla^2 u + \lambda u(1-u), \tag{13}$$

which has the same steady-state solutions as (2) but different stability properties. As no delay terms occur in (13) its steady-state solutions are stable for all parameter values. Hence it is an appropriate model to generate steady-state solutions of (2), for all values of λ and all choices of f. There is an excellent comparison between the two-term semi-analytical and numerical solutions, with only a 2.7% error at $\lambda = 30$.

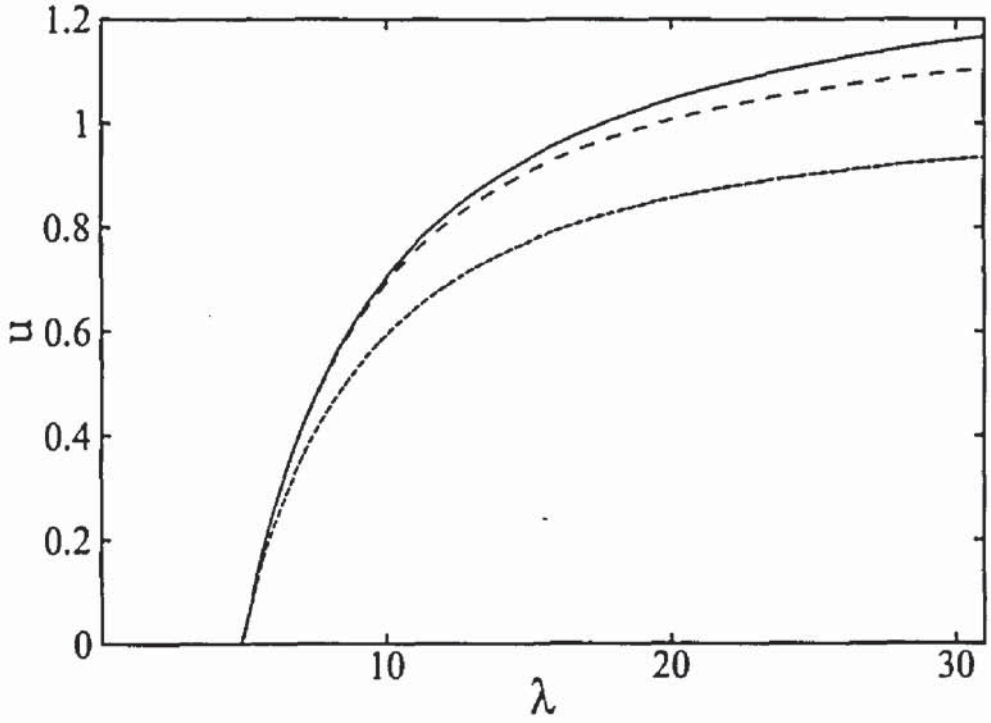

Figure 2: The steady-state population density u, at $x = y = 0$, for the two-dimensional model. Shown is the one-term (solid line) and two-term (long dashes) semi-analytical solutions of (2) and numerical (small dashes) solution of (13).

Figure 2 shows the steady-state population density u at the centre of the domain, $x = y = 0$, for the two-dimensional model. As in one-dimensional case, the one and two-term semi analytical solutions of (2) and numerical solutions are shown. The curves are qualitatively similar to figure 1 but the difference between the semi-analytical and numerical solutions is slightly larger, for large λ. The difference between the numerical and two-term semi-analytical solutions is 15% at $\lambda = 30$. Two-dimensional problems generally

are a more severe test of the semi-analytical method, producing slightly larger errors, see [14].

5 Stability analysis and Hopf bifurcations

In this section we consider the stability of the non-uniform steady-state solutions and determine the Hopf bifurcation points. A Hopf bifurcation denotes the appearance of periodic solutions in the neighborhood of a steady state whose stability changes, due to the crossing of a conjugate pair of eigenvalues over the imaginary axis, see [16]. The theory of Hopf bifurcations for delay systems is described in texts on bifurcation theory and dynamical systems, for further details see [4, 9]. The delay ode models are used to find a semi-analytical approximation for the parameter region, in which periodic solutions occur.

5.1 Hopf bifurcation for the delay ode models

Hopf bifurcation points are obtained, for the one and two-dimensional geometries, for the three different delay models. The one-dimensional geometry models consists of two odes, for u_0 and u_1. These are expanded in a Taylor series about the steady-state solution. We let

$$\begin{aligned} u_0 &= u_{0s} + \epsilon f e^{-\mu t}, \quad & v_0 &= u_{0s} + \epsilon f e^{-\mu t} e^{\mu \tau}, \\ u_1 &= u_{1s} + \epsilon g e^{-\mu t}, \quad & v_1 &= u_{1s} + \epsilon g e^{-\mu t} e^{\mu \tau}, \end{aligned} \tag{14}$$

and substitute this into the odes of system (8), and linearize around the steady state. The eigenvalues of the Jacobian matrix describes the growth of a small perturbation in the system. For instance, the determinant of the Jacobian matrix, in the point delay case, is $q = |F_1 G_2 - F_2 G_1|$ where,

$$\begin{aligned} F_1 &= \lambda - \frac{\pi^2}{4} - \frac{8}{3\pi}\lambda u_{0s} e^{\mu\tau} - \frac{8}{3\pi}\lambda u_{0s} - \frac{8}{15\pi}\lambda u_{1s} - \frac{8}{15\pi}\lambda u_{1s} e^{\mu\tau} + \mu, \\ G_2 &= \frac{\lambda}{\pi} - \frac{9\pi^2}{4} - \frac{70}{\pi}\lambda u_{1s} e^{\mu\tau} - \frac{70}{\pi}\lambda u_{1s} + \frac{162}{\pi}\lambda u_{0s} + \frac{162}{15\pi}\lambda u_{0s} e^{\mu\tau} + \mu, \\ F_2 &= \frac{162}{\pi}\lambda u_{1s} e^{\mu\tau} - \frac{8}{15\pi}\lambda u_{0s} e^{\mu\tau} - \frac{8}{15\pi}\lambda u_{0s} + \frac{162}{\pi}\lambda u_{1s}, \\ G_1 &= -\frac{8}{15\pi}\lambda u_{0s} e^{\mu\tau} - \frac{72}{35\pi}\lambda u_{1s} e^{\mu\tau} - \frac{72}{35\pi}\lambda u_{1s} - \frac{8}{15\pi}\lambda u_{0s}. \end{aligned} \tag{15}$$

Now $q = 0$ represents a characteristic equation for μ, the growth rate. We let $\mu = iw$ in this characteristic equation and separate the real and imaginary parts, termed q_1 and q_2 respectively, of the characteristic equation $q = 0$. A Hopf bifurcation is born at points where μ is purely imaginary. Hence, we look for real solutions to the system of equations

$$q_1 = q_2 = f_1 = f_2 = 0. \tag{16}$$

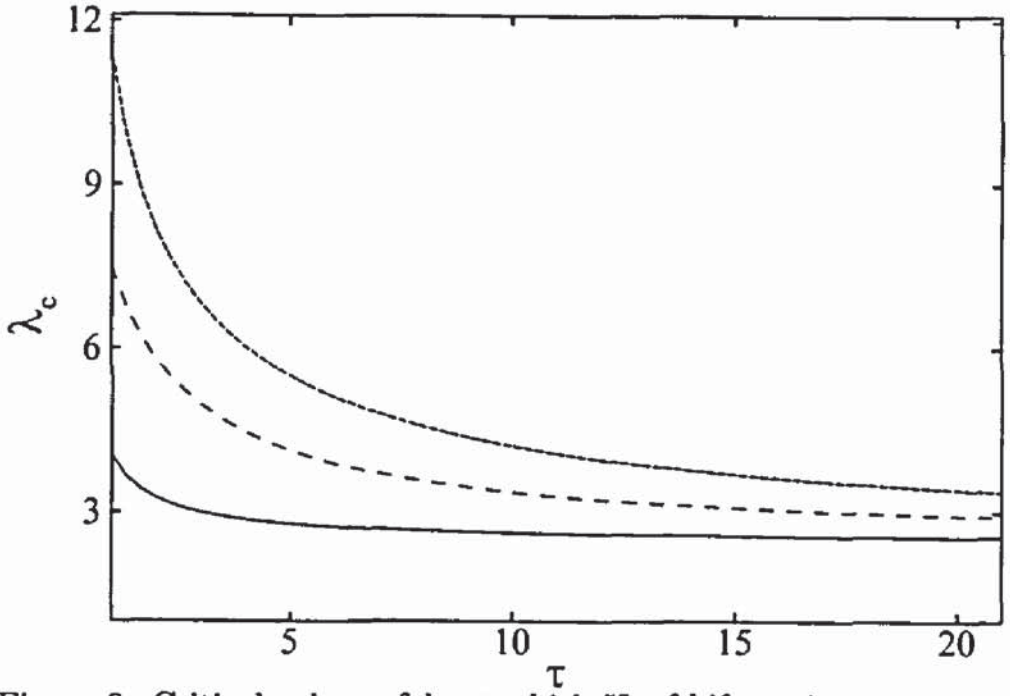

Figure 3: Critical values of λ, at which Hopf bifurcations occur in the one-dimensional geometry. Shown are the point delay (solid line), uniformly weighted delay (long dashes) and exponentially weighted delay (small dashes) cases.

The characteristic equations for the uniformly weighted and exponentially weighted cases are not shown but are qualitatively similar to (15).

Figure 3 shows the Hopf bifurcation points, λ_c versus τ, for the one-dimensional geometry, for the three delay models considered. Shown are the point delay case and uniformly and exponential weighted delays. The time interval over which feedback occurs is $[t, t-\tau]$, hence increasing the delay parameter τ increases the size of the feedback window and the contributions from the more distant past. The figure shows that as the delay parameter τ increases, that the critical value of λ, at which Hopf bifurcations first occur, decreases. This implies that increasing the feedback from the more distant past destabilizes the system, hence reducing the parameter region in which stable solutions occur. The figure also shows that, for fixed τ, the exponential weighted delay case has the largest region of stability, followed by the uniformly weighted case, with the point delay case having the smallest region of stability. The relative stabilities of the three delay examples considered here can be understood by considering the relative contribution of the outer edge of the feedback interval, at time $t-\tau$. In the point delay case all the feedback is from this outer edge, at time $t-\tau$. In the uniformly distributed delay case it plays a lesser role, while it plays almost no role in the exponentially distributed case. This again implies that increased feedback, from the more distant past, destabilizes the system.

We now consider some comparisons for the special case when the delay

parameter $\tau = 1$. The numerically obtained Hopf bifurcation points are $\lambda_c = 4.04$, 7.48 and 11.3 for the point delay, uniformly distributed delay and exponentially distributed delay cases, respectively. The predictions of the two-term semi-analytical theory are the same as the numerical predictions, to three significant figures, hence the semi-analytical theory is an excellent predictor of the occurrence of Hopf bifurcations.

The technique for finding Hopf bifurcation points in the two-dimensional geometry is similar to the one-dimensional case. We solve the system of equations

$$q_1 = q_2 = f_1 = f_2 = f_3 = 0 \tag{17}$$

where q_1 and q_2 are again the real part and imaginary parts of the appropriate characteristic equation. The numerically obtained Hopf bifurcation points for $\tau = 1$ are $\lambda_c = 6.50$, 9.84 and 13.6 for the point delay, uniformly distributed delay and exponentially distributed delay cases, respectively. The two-term semi-analytical predictions, for the occurrence of Hopf bifurcation points, are 6.52, 9.97 and 13.8. Hence the semi-analytical predictions are excellent for the two-dimensional geometry, with a maximum error of 1.5%.

For the simple one-term semi-analytical theory λ_c increases by $\frac{\pi^2}{4}$ as the dimension of the geometry is increased, from zero (the case of no diffusion), to one and two-dimensions, in turn. The more accurate two-term semi-analytical solutions, and the numerical solutions, presented here, also obey this rule, in an approximate sense. The results presented here, show that λ_c increases by approximately $\frac{\pi^2}{4} \approx 2.5$, as the geometry (and the diffusive effects) change from one to two-dimensions.

6 Bifurcation diagrams and transient solutions

Bifurcation diagrams and transient solutions are now considered, for various parameter choices, with comparisons made between semi-analytical and numerical solutions. The fourth-order Runge Kutta method is used to find the solutions of the semi-analytical ode models. All the examples in this section use the parameters $\tau = 1$ and $u_a = 0.5$. Note that the bifurcation diagrams display long time solutions, of the steady-state amplitude and the maximum and minimum amplitudes of the periodic oscillations, so are not functions of the initial population u_a. Also the bifurcation diagrams show the populations at the centre of the one and two-dimensional geometries; the same bifurcation diagram (with an amplitude scaling) occurs at different locations within the solution domain.

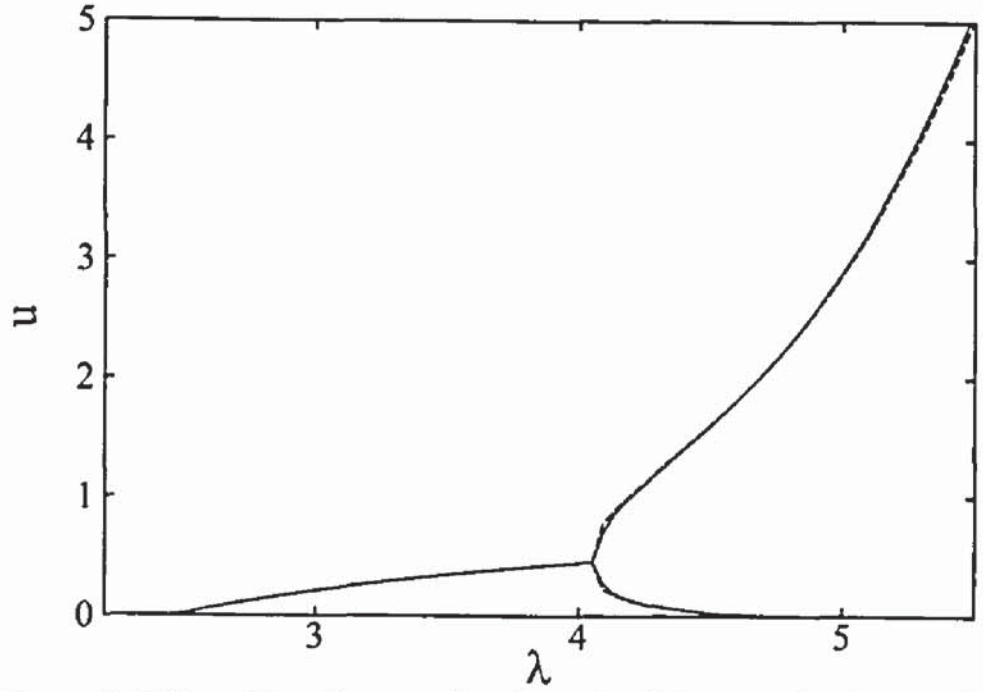

Figure 4: Bifurcation diagram for the point delay case in the one-dimensional geometry, with $\tau = 1$. The two-term semi-analytical solutions (solid line) and numerical solution (dashed line) are shown. A supercritical Hopf bifurcation appears at $\lambda_c \simeq 4.04$. After the Hopf point, the maximum and minimum amplitudes of the periodic solution are shown.

6.1 One-dimensional geometry

Figures 4, 5 and 6 are the bifurcation diagrams for the one-dimensional geometry, with $\tau = 1$, for the point, uniformly distributed and exponentially distributed delays, respectively. The two-term semi-analytical and numerical solutions are shown. The solutions are stable for $\frac{\pi^2}{4} < \lambda < \lambda_c$. A supercritical Hopf bifurcation occurs at λ_c and periodic solutions occur for parameter values larger than this. In the region where periodic solutions occur the maximum and minimum amplitudes of the oscillations are shown. The supercritical Hopf bifurcation occurs at $\lambda_c = 4.04$, 7.47 and 11.4, for the point, uniformly distributed and exponentially distributed delays, respectively. The discussion for figure 3 explains the reasons why λ_c is smallest for the point delay case and largest for the exponentially distributed delay case. It can be seen that in all three cases that the two-term semi-analytical solutions are extremely accurate in both the stable and oscillatory regimes of the bifurcation diagram, with the curves nearly the same, to graphical accuracy. The maximum difference between the solutions increases slowly as λ increases, but is no greater than 2%, for the parameter ranges shown in the figures. A feature of the periodic solution for the delay logistic equation (1) is that the minimum amplitude is doubly exponentially small, see [6]. The same qualitative feature is evident here, for the minima of the oscillations.

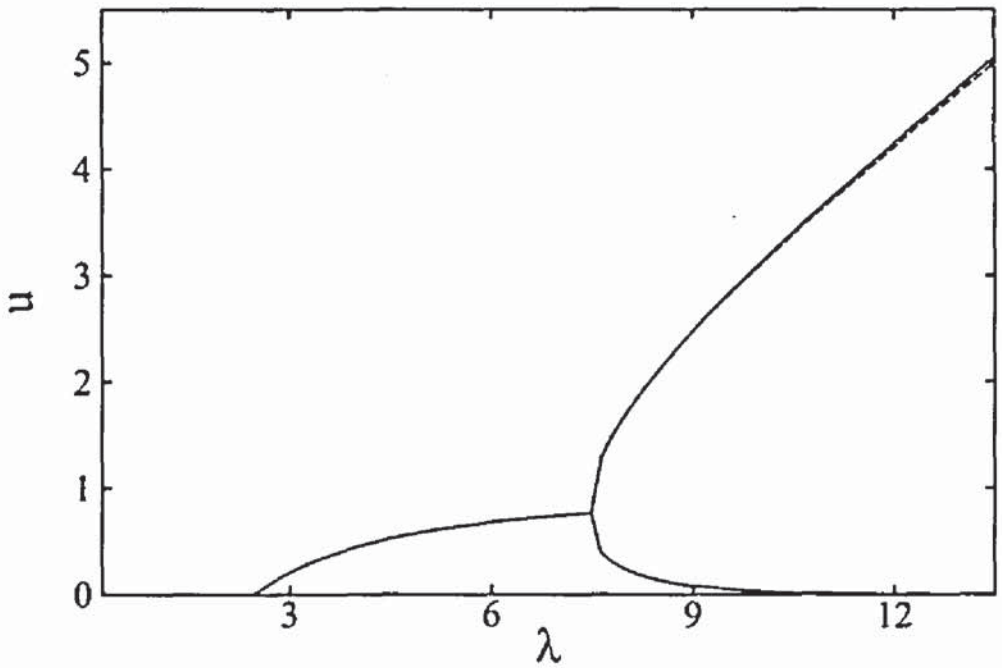

Figure 5: Bifurcation diagram for the uniformly distributed delay in the one-dimensional geometry, with $\tau = 1$. The two-term (solid line), semi-analytical solutions and numerical solution (dashed line) are shown. A supercritical Hopf bifurcation appears at $\lambda_c \simeq 7.47$.

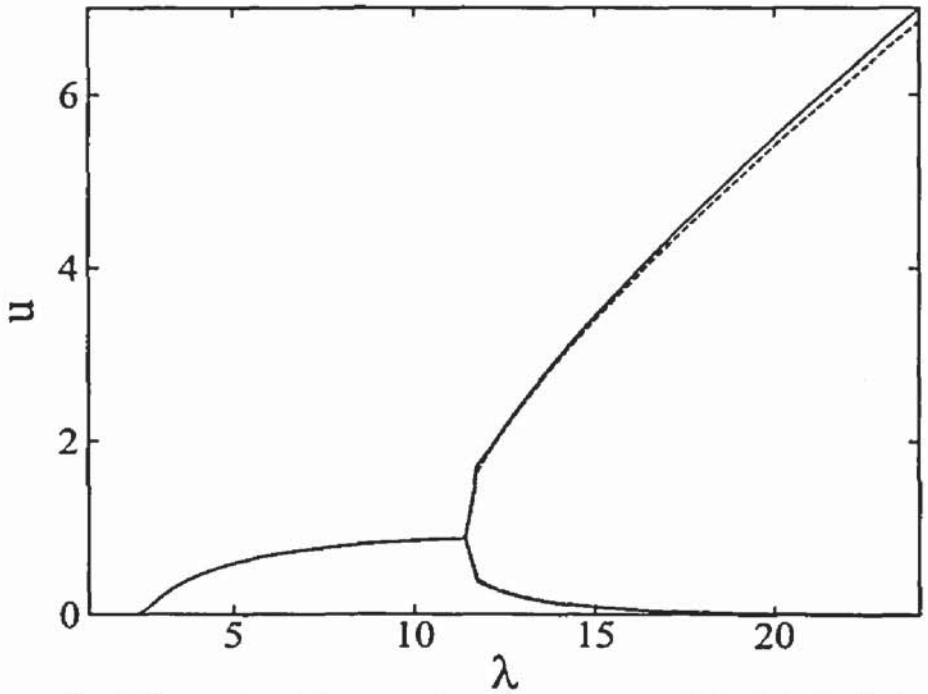

Figure 6: Bifurcation diagram for the exponential distributed delay in the one-dimensional geometry, with $\tau = 1$. The two-term (solid line), semi-analytical solutions and numerical solution (dashed line) are shown. A supercritical Hopf bifurcation appears at $\lambda_c \simeq 11.4$.

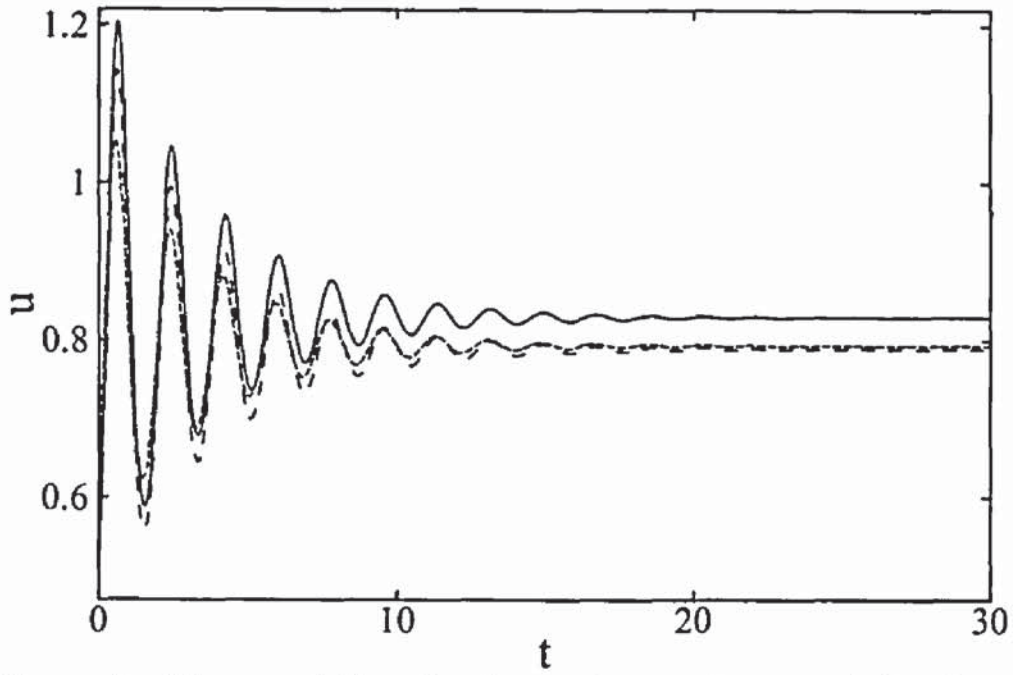

Figure 7: The population density u at $x = 0$ versus t for the exponential distributed delay in the one dimensional geometry. The one-term (solid line), two-term (long dashes) semi-analytical solutions and numerical solution (small dashes) are shown. The parameters are $\lambda = 9$, $u_a = 0.5$ and $\tau = 1$.

Figures 7 and 8 show the population density u at $x = 0$ versus t for the exponentially distributed delay, in the one-dimensional geometry. The parameters are $u_a = 0.5$ and $\tau = 1$, with $\lambda = 9$ for figure 7 and $\lambda = 13$ for figure 8. The one and two-term semi-analytical and numerical solutions are shown. For figure 7 $\lambda = 9 < \lambda_c \simeq 11.4$ and the solution evolves to a steady-state, with $u(0,t) \simeq 0.79$ as the time becomes large, after some initial relaxation oscillations. The comparison between the two-term semi analytical and numerical solutions is excellent with only a 0.6% error at $\lambda = 30$. The difference between the numerical solution and the one-term semi-analytical solution is slightly higher, being 4.33% at $\lambda = 30$. For figure 8 $\lambda = 13 > \lambda_c$ and periodic solutions occur. The numerical period and amplitude of the limit cycle are 1.51 and 2.42, respectively. These values are very close to the two-term semi-analytical period and amplitude, 1.51 and 2.44, respectively. The errors in the two-term semi-analytical values are less than 1%.

6.2 Two-dimensional geometry

Figures 9, 10 and 11 are the bifurcation diagrams for the two-dimensional geometry, with $\tau = 1$ for the point, uniformly distributed and exponentially distributed delays, respectively. The two-term semi-analytical and numerical solutions are shown. The solutions are stable for $\frac{\pi^2}{2} < \lambda < \lambda_c$. A

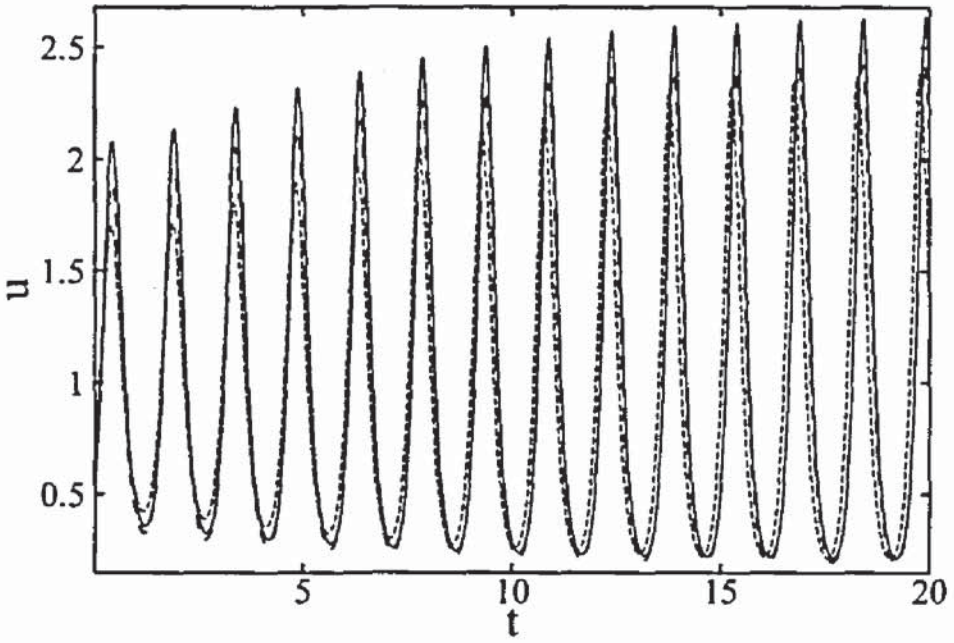

Figure 8: The population density u at $x = 0$ versus t for the exponential distributed delay in the one-dimensional geometry. The one-term (solid line), two-term (long dashes) semi-analytical solutions and numerical solution(small dashes) are shown. The parameters are $\lambda = 13$, $u_a = 0.5$ and $\tau = 1$.

supercritical Hopf bifurcation occurs at λ_c and periodic solutions occur for parameter values larger than this. The supercritical Hopf bifurcation occurs at $\lambda_c = 6.52$, 9.97 and 13.8, for the point, uniformly distributed and exponentially distributed delays, respectively. The bifurcation diagrams for the two-dimensional geometry are qualitatively similar to their one-dimensional counterparts. The comparison between the two-term semi-analytical and numerical solutions is very good, but some differences occur for large λ. This reflects the fact, mentioned earlier, that two-dimensional geometries are a more significant test of the semi-analytical method, than one-dimensional geometries. The difference between the maximum amplitude of the periodic solution, as predicted by the two-term semi analytical and numerical solutions, is up to 15%, for the range of λ shown in the figures.

Figures 12 and 13 show the population density u at $x = y = 0$ versus t for the point delay case, in the two-dimensional geometry. The parameters are $u_a = 0.5$ and $\tau = 1$ with $\lambda = 6$ for figure 12 and $\lambda = 7$ for figure 13. The one-term, two-term semi-analytical solutions and numerical solutions are shown. For figure 12 $\lambda = 6 < \lambda_c \simeq 6.52$ and the solution evolves to a steady-state, with $u(0, 0, t) \simeq 0.25$ as the time becomes large. The comparison between the numerical and the two-term semi-analytical solutions is very good with a 12% difference at the steady-state. For figure 13 $\lambda = 7 > \lambda_c$ so periodic solutions occur. The numerically obtained period and amplitude are 4.53

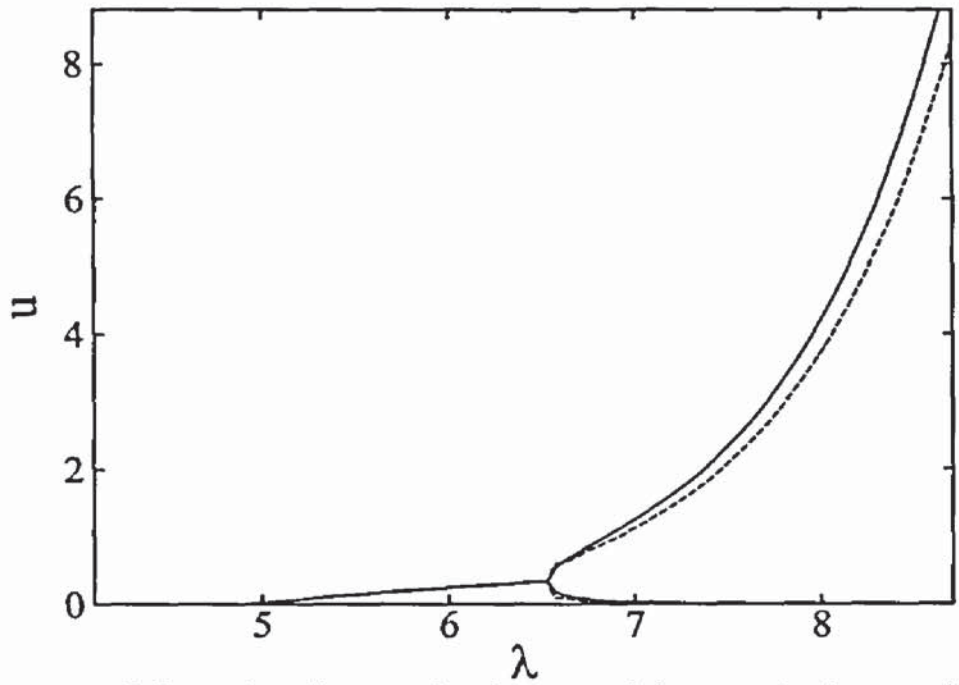

Figure 9: Bifurcation diagram for the point delay case in the two-dimensional geometry, with $\tau = 1$. The two-term semi-analytical solutions (solid line) and numerical solution (dashed line) are shown. A supercritical Hopf bifurcation appears at $\lambda_c \simeq 6.52$.

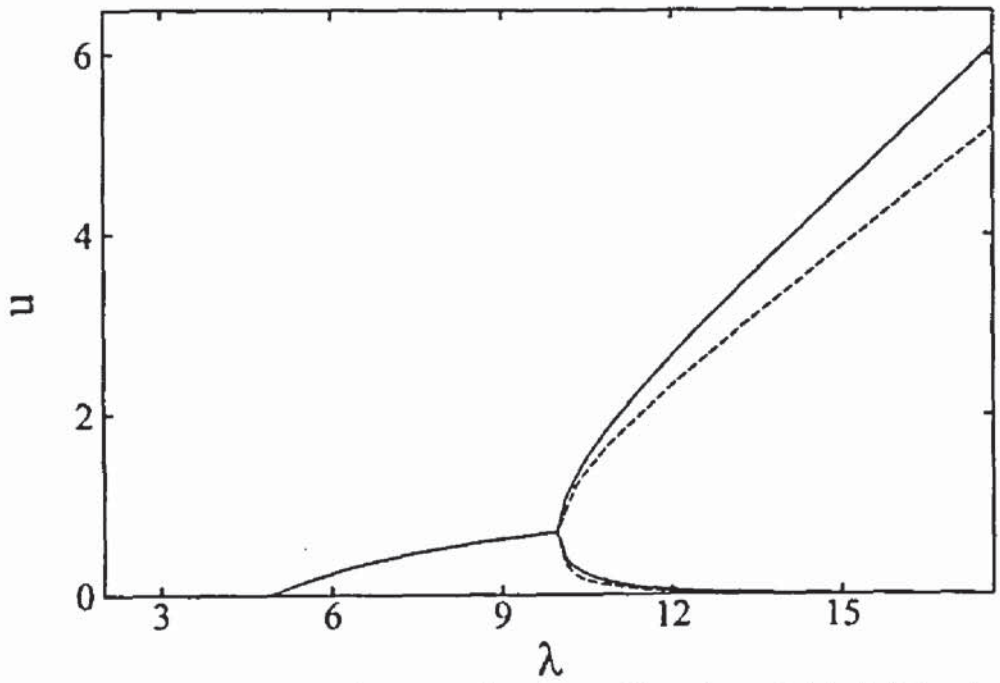

Figure 10: Bifurcation diagram for the uniformly weighted delay in the two-dimensional geometry, with $\tau = 1$. The two-term semi-analytical solutions (solid line) and numerical solution (dashed line) are shown. A supercritical Hopf bifurcation appears at $\lambda_c \simeq 9.97$.

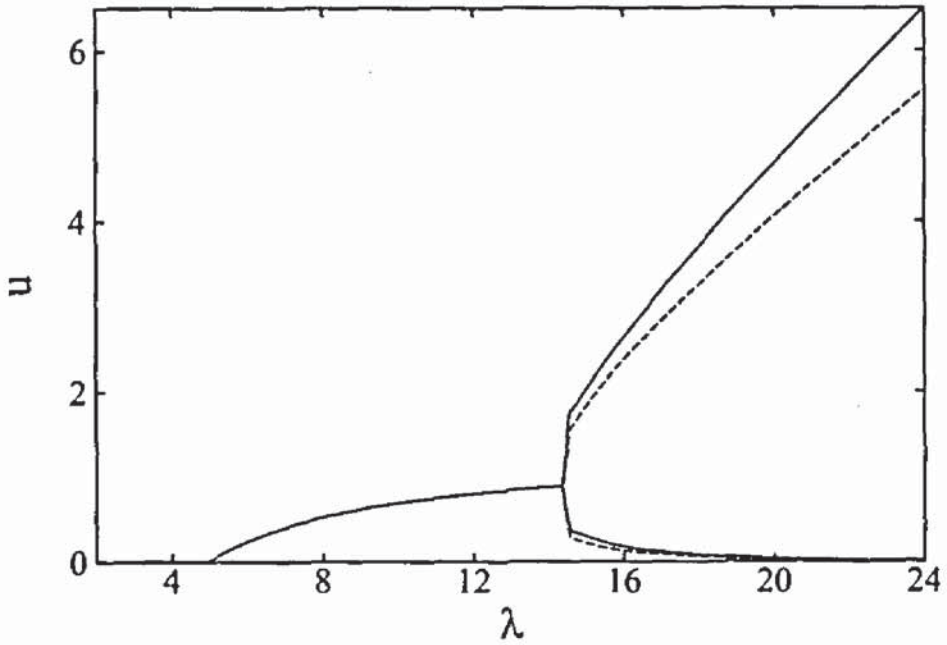

Figure 11: Bifurcation diagram for the exponential distributed delay in the two-dimensional geometry, with $\tau = 1$. The two-term semi-analytical solutions (solid line) and numerical solution (dashed line) are shown. A supercritical Hopf bifurcation appears at $\lambda_c \simeq 13.8$.

and 1.25, respectively, while the two-term semi-analytical estimates are 4.46 and 1.13. The two-term semi-analytical method is again extremely accurate with errors of less than 10%.

7 Conclusions

This paper has presented semi-analytical solutions for a class of generalised diffusive logistic delay equations, with both distributed and point delays. The semi-analytical model allowed the governing pdes to be approximated by an ode model, allowing a stability analysis to be performed. Bifurcation diagrams, transient solutions and Hopf bifurcation points were found, for both one and two -dimensional geometries. A good comparison between semi-analytical and numerical solutions was found. It can be concluded that the semi-analytical method is an useful and accurate analytical technique, for pde systems with delay. Future work will apply the semi-analytical method developed here to other reaction-diffusion-delay systems, such as Nicholson's blowfly equations model.

Acknowledgement. Hassan Alfifi gratefully acknowledges the Saudi government and the University of Dammam (Saudi Arabia) for the awarding of a PhD Scholarship. The authors also wish to thank an anonymous referee for their useful comments.

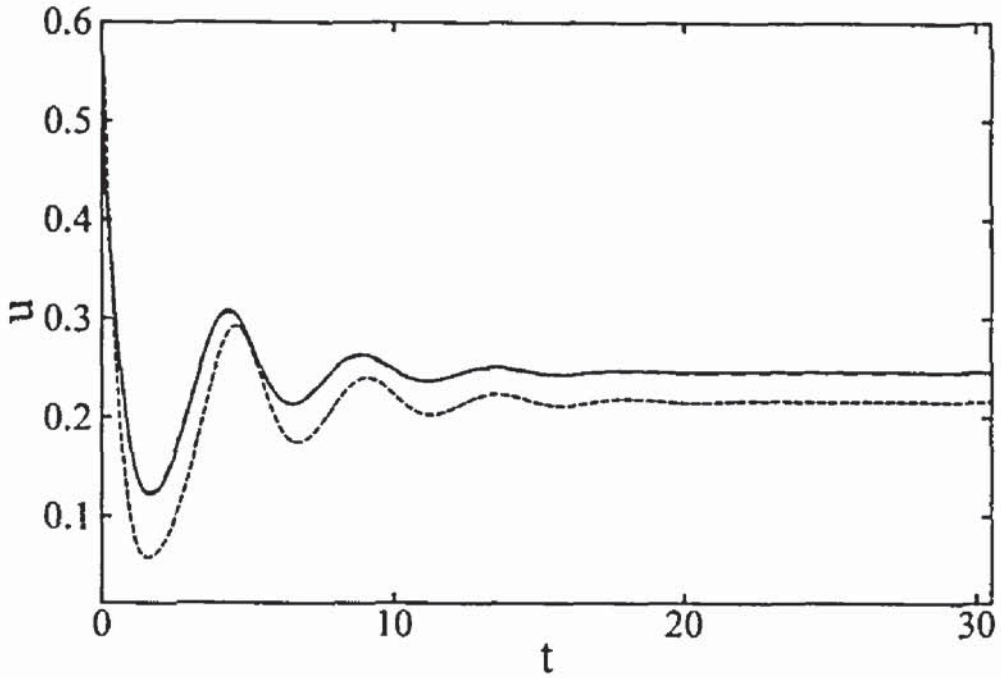

Figure 12: The population density u at $x = y = 0$ versus t for the point delay case in the two-dimensional geometry. The one-term (solid line), two-term (long dashes) semi-analytical solutions and numerical solution (small dashes) are shown. The parameters are $\lambda = 6$, $u_a = 0.5$ and $\tau = 1$.

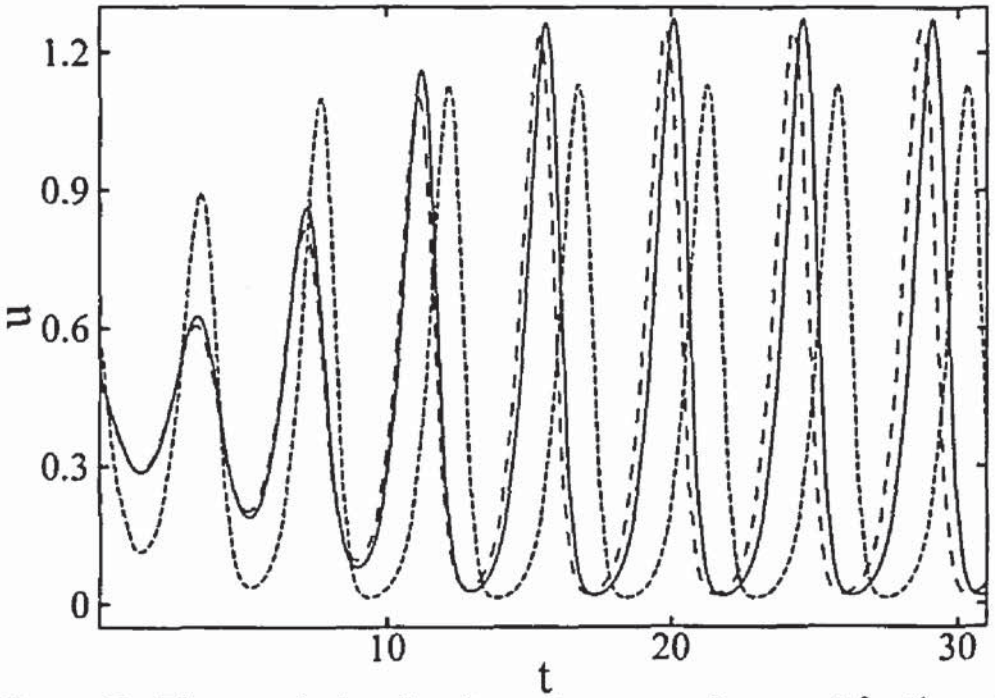

Figure 13: The population density u at $x = y = 0$ versus t for the point delay case in the two-dimensional geometry. The one-term (solid line), two-term (long dashes) semi-analytical solutions and numerical solution (small dashes) are shown. The parameters are $\lambda = 7$, $u_a = 0.5$ and $\tau = 1$.

References

[1] M. Adimy, F. Crauste, and S. Ruan. Stability and Hopf bifurcation in a mathematical model of pluripotent stem cell dynamics. *Nonlinear Anal-Real.*, 6:651–670, 2005.

[2] H. T. Banks, D. M. Bortz, and S. E. Holte. Incorporation of variability into the modeling of viral delays in HIV infection dynamics. *Math. Biol.*, 183:63-91, 2003.

[3] E. Beretta, R. Kon, and Y. Takeuchi. Nonexistence of periodic solutions in delayed Lotka-Volterra systems. *Nonlinear Anal-Real.*, 3:107–129, 2002.

[4] T. Erneux. *Applied Delay Differential Equations.* Springer, New York, 2009.

[5] W. Feng and X. Lu. On diffusive population models with toxicants and time delays. *J. Math. Annal*, 233:373–386, 1999.

[6] A. C. Fowler. An asymptotic analysis of the delayed logistic equation when the delay is large. *IMA J. Appl. Maths.*, 28:41–49, 1982.

[7] A. C. Fowler. Asymptotic methods for delay equations. *J. Engng. Maths*, 53:271–290, 2005.

[8] S. A. Gourley and S. Ruan. Dynamics of the diffusive Nicholson's blowflies equation. *Proc. Roy. Soc. Edin. Sect. A*, 130A:1275–1291, 2000.

[9] J. Hale. *Theory of Functional Differential Equations.* Springer Verlag, New York, 1977.

[10] G. E. Hutchinson. Circular causal systems in ecology. *Ann. New York Acad. Sci*, 50:221–246, 1948.

[11] J. J.W.-H So, J. Wu, and Y. Yang. Numerical steady state and Hopf bifurcation analysis on diffusive Nicholson's blowflies equation. *App. Math. Comput.*, 111:33–51, 2000.

[12] Y. N. Kyrychko and S. J. Hogan. On the use of delay equations in engineering applications. *J. Vib. Control*, 16:943-946, 2010.

[13] T. R. Marchant. Cubic autocatalytic reaction diffusion equations: semi-analytical solutions. *Proc. R. Soc. Lond.*, A458:873–888, 2002.

[14] T. R. Marchant and M. I. Nelson. Semi-analytical solution for one-and two-dimensional pellet problems. *Proc. R. Soc. Lond.*, A460:2381–2394, 2004.

[15] H. Rasmussen, G. C. Wake, and J. Donaldson. Analysis of class of distributed delay logistic differential equations. *Math. Comput. Modelling*, 38:123–132, 2003.

[16] G. D. Smith. *Numerical Solution of Partial Differential Equations: Finite Difference Methods.* Oxford, New York, third edition, 1985.

[17] Y. Su, J. Wei, and J. Shi. Hopf bifurcations in a reaction diffusion population model with delay effect. *J. Differ. Equations*, 247:1156–1184, 2009.

[18] T. Suebcharoen, P. Satiracoo, and G. C. Wake. Distributed delay logistic equations with harvesting. *Differential Integral Equations*, 22:321–337, 2009.

[19] S. Yuan, Y. Song, and M. Han. Direction and stability of bifurcating periodic solutions of a chemostat model with two distributed delays. *Chaos Solitons Fract.*, 21:1109-1123, 2004.

[20] Z. Zhao, Q. Song, and Y. Li. Global exponential stability and existence of periodic oscillatory solutions for reaction-diffusion genralized neural networks with time-varying delays. *Dynam. Cont. Dis. Ser. B*, 14:371–384, 2007.

Received October 2010; revised January 2011; revised September 2011.

email: journal@monotone.uwaterloo.ca
http://monotone.uwaterloo.ca/~journal/